Article

Sustainable Coating Materials: Exploring the Influence of Adjuvants on Kaolinite Suspension with Insights from Five Local Mining Clays

Nalinthip Chanthaset,* Nichagarn Greetatorn, Oratai Jongprateep, Hiroharu Ajiro,* and Kanapol Jutamanee*

Read Online

ACCESS | Metrics & More | Article Recommendations | Supporting Information

ABSTRACT: Herein, we presented a comprehensive case study on the kaolin suspension derived from mining powder, with a specific emphasis on its mineral constituents within the size range of 2−5 μm and its suitability in spray applications. We have systematically investigated the influence of adjuvants, existing in both organic molecules and polymers, on the sedimentation behavior of clay suspensions. The investigations included the analysis of turbidity, dispersion weight, pH, and surface charge as key parameters. Our findings revealed that the specific presence of PEG−PPG-PEG, PAA, and PSAMA had a notable effect on delaying the suspension of sedimentation by the actual sediment weight as well as enhancing the uniformity of clay coating by the reflection efficiency of coating materials in PPFD units. To enhance sustainability in coating materials, it was essential to elucidate the optimal amounts of adjuvants and the pH levels as they are closely related to the efficacy of tree-coated spraying and soil conditions.

1. INTRODUCTION

Global warming raises concerns of excessively high temperature and sunburn, impacting fruit yield and quality.[1,2] Addressing this challenge, sustainable clay suspension is essential in fruit tree cultivation.[3,4] With benefits like light reflection, heat stress mitigation, and disease protection, clay solution offers promises especially its low thermal conductivity provides insulation.[5−7] When applied as a foliar spray, the mineral clay particle forms a reflective layer on leaves, reducing water loss, preserving moisture, and preventing sunburn, particularly valuable in arid regions.[8,9]

Kaolinite $(Al_2Si_2O_5(OH)_4)$, the most abundant phyllosilicate group clays, comprises mainly silicate sheets (Si_2O_5) bound to aluminum oxide/hydroxide layers $(Al_2(OH)_4)$, which is vital in ceramics and agriculture.[10,11] However, its sedimentation behavior in water limits its effectiveness, causing the rapid precipitation of inorganic particles.[12] The primary factors influencing sedimentation are the self-weight of coarse-grain particles and the electrostatic force acting on fine-grain particles.[13] Previous research attempted direct modification of kaolin particles or kaolin intercalation compounds but faced the unfeasible issues of large-scale production, high costs, time-consuming procedures, and overall complexity. Functionalization of the interlayer surfaces of kaolinite by grafting such as alkylammonium,[14] polyols,[15] porphyrin,[16] polymethacrylate,[17] poly(acrylic acid),[18] alkanols, diols, glycol monoethers, dimethyl sulfoxide, and alkyl chain length[16] have been reported. The mandatory is for ionic liquids, deintercalation-

hydrolysis resistance, and adsorption sites. Nevertheless, the blending of diverse natural or synthetic polymers such as chitosan, poly(ethylene oxide), sodium laurate sulfate, and polyacrylamide have been blended with kaolinite to improve physicochemical and mechanical properties,[19] clay−polymer system,[20] and sedimentation behavior.[19,21] However, the potential utilization of clay for agricultural purposes has yet to be fully realized. Plus, commercially available blend surfactants are numerous, and the commercial may not directly address the specific clay problem at hand.[22] To address this, numerous researchers have paid attention to the study of the electrokinetic properties of clay minerals.[23] The kaolinite structure is represented by hexagonal platelets with predominantly negatively charged faces (SiO_2) and positively charged edges (Al_2O_3), which electrostatic charge is the overall negative in aqueous.[24] The zeta potential (ZP) of a kaolinite suspension ranged from −25 mV at pH 3 to −42 mV at pH 11. The clay surface exhibited a more negative ZP with higher pH levels and in the presence of NaCl and LiCl solution compared to water.[25] Moreover, the sedimentation behavior of kaolinite platelets exhibited notable variations in response to fluctua-
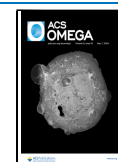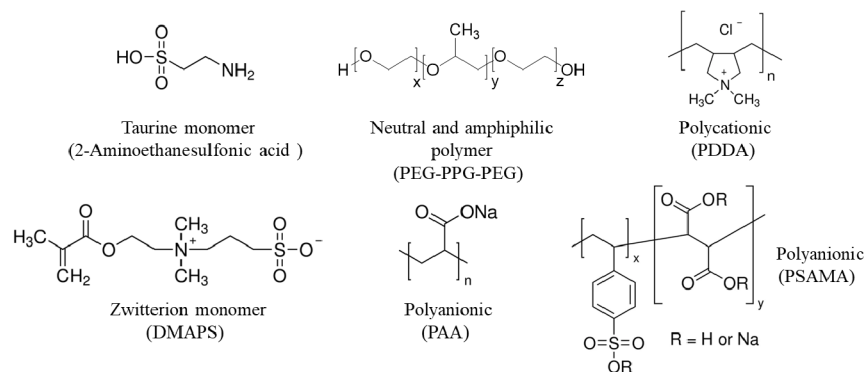
Figure 1. Chemical structure of molecules and polymeric adjuvants in this study.

tions in environmental salt ion and pH. The microstructure study findings revealed differences in the compactness of clay orientation, with a distinct order observed in salt (kaolin book), alkaline (face-to-face repulsion), water, and acidic condition (randomly face-to-face).[26,27]

As sustainable application of the mining clay solution, it was reported that spraying kaolin on tree leaves and fruits from early stages until it is fully grown has been shown to effectively reduce anthracnose and fruit rot after harvesting. Therefore, the economical benefit of kaolin as a fruit coating material is its ability to enhance fruit quality by reducing fruit diseases during ripening and prolonging the fruit shelf life.[28] Another concern for spray application is the pH impact on fruit plant surface and soil. As healthy citrus, it is noteworthy that a pH 8.0 in both water and soil resulted in the highest rates of mortality and leaf drop in comparison to pH 5.8. Additionally, pH 8.0 led to reduced plant height growth and lower leaf biomass compared to the promising pH 6.0.[29] Therefore, it is essential to maintain an optimal pH range for citrus growth, which typically falls within the spectrum of mild acidity. Furthermore, plant photosynthesis is often assessed using "Photosynthetic Photon Flux Density" (PPFD), measuring active photosynthetic photons per second per square meter (μmol/s/m^2).[30] A healthy *Citrus sinensis* (L.) Osbeck (orange tree) exhibits a light saturation point of PPFD between 600 and 1000 μmol/s/m^2 and an optimal temperature of 35 °C for crucial parameters such as photosynthesis rate and others.[30−34]

This study represents the exploration into the impact of the polymeric adjuvant category on kaolinite suspension, with an initial focus on observing suitable light reflection (PPFD) when the suspensions were coated. Also, the characterization of commercially available fine clays and regionally mined kaolin were investigated their mineral phase fractions, microstructures, surface charge behavior and sediment weight in aqueous with timing assessment. In terms of sustainability, the pH value of the clay suspensions was elucidated with the aim of mitigating any adverse effects on plants and soil.

2. EXPERIMENTAL SECTION

2.1. Materials. 2-Aminoethanesulfonic acid (taurine), poly(ethylene glycol)-*block*-poly(propylene glycol)-*block*-poly-(ethylene glycol) (Pluronic F-108, PEG−PPG-PEG, M_n ∼ 14600), anionic polymer; poly(4-styrenesulfonic acid-co-maleic acid) sodium salt (PSAMA, M_w ∼ 20000), poly(acrylic acid sodium salt) (PAA, M_w ∼ 5,100), cationic polymer; and poly(diallyldimethylammonium chloride) solution (PDDA, M_w 200,000−350,000) were purchased from Sigma-Aldrich.

Zwitterionic monomer and 3-[[2-(Methacryloyloxy)ethyl]-dimethylammonio]propane-1-sulfonate (DMAPS) were purchased from Tokyo Chemical Industry Co. Ltd., Japan. All molecules and polymers were utilized without purification processes. The samples of kaolinite clay were provided by our collaborators from the Department of Botany, Faculty of Science, Kasetsart University, Bangkok, and were appropriately labeled according to their respective regional sources. The X-ray diffraction analysis revealed that clays were sourced from MaeThan (MT), Ranong (RN), Lampang (LP), Ceramic-Lampang (C-LP), and Narathiwat (NRTW) along with commercially available clays known as Imerys and SCG Figure 1.

2.2. Measurement. Proton nuclear magnetic resonance spectroscopy (^{1}H NMR) was recorded using a JEOL JNM-ECX400 instrument at 400 MHz with tetramethyl silane (TMS) as an internal standard. Fourier transform infrared (FT-IR) spectrometer spectra were obtained with IR Affinity-1S Shimadzu. The phase identification of kaolin powders was conducted using an X-ray diffractometer (XRD, Paralytical, Empyrean), while sample microstructural was examined via scanning electronmicroscopy (SEM; Philips XL30) and the particle size of the powders via ImageJ software.

The electric charge on the particle's surface was determined by dynamic light scattering (DLS) Malvern ZEN 3600 Zetasizer NANO-ZS (UK, He Ne laser, 633 nm, limitation range 3 nm −10 μm). The sedimentation rate of clay was measured by UV-2600 (Shimadzu Corporation, Japan) at 450 nm with a D-51588 type cell.

The determination of weight content was carried out by using BAS 31 plus Balances (Boeckel & Co. GmbH & Co. KG, Germany), VGT-2013QT Ultrasonic cleaner (Guangdong GT Ultrasonic Co., Ltd., China), and AREC Heating Magnetic Stirrer (VELP China Co. Ltd., China). The measurement of the reflection efficiency of the coating material was conducted by using LI-190R Quantum Sensor (LI-COR, Inc., Nebraska, USA) connected to Campbell Scientific datalogger CR-1000 and displayed the PAR on Loggernet. Light source for this experiment was spotlight mode of 18 V LXT L.E.D. Flashlight/Spotlight (DML812) (Makita, USA). The measurement of pH was conducted by pH100 pH meter (IONIX Instruments Pte, Ltd., Singapore)

2.3. Clay Powder Characterization. *2.3.1. Mineral Phase Identification and Microstructure Determination.* The mineral phase identification of kaolin powders was conducted by XRD over a 2θ angle ranging from 5° to 80° with a step size of 0.0261°, while sample microstructure was

examined via SEM with accelerating 5000 voltage and SE mode. The ImageJ software was used in the analysis of the particle size of the powders.

To analyze the organic residue, 100 mg of kaolin clay was dissolved in $CDCl_3$ and DMSO-d_6 0.75 mL, separately. The supernatants were measured by ^1H NMR spectroscopy at room temperature.

2.4. Sedimentation Behavior (Turbidity). The solution of samples was prepared at concentrations of 10, 20, and 30 mg/mL, and each 2 mL was picked up for measurement. Then, they were measured the transmittance intensity by UV−vis spectroscopy at 450 nm for 0——40 min. The plotting of transmittance percentage was compromised with the optimum sedimentation rate by setting cuvette cell containing DI water 2 mL as 100% transmittance.

2.5. Weight Content of Suspension. A 30 g/L concentration of kaolin clay suspension from MT was prepared with individual adjuvants dissolved through sonication. We determined the following concentrations: 0.5 M for taurine and DMAPS, 0.1, 1, and 3 g/L for neutral polymers, and 1 g/L for both anionic and cationic polymers each. Furthermore, we combined two adjuvants by mixing neutral polymers, PEG−PPG-PEG, and anionic polymers, such as PAA or PSAMA, at concentration ratios of 0.5 g/L: 0.5 g/L and 1 g/L: 1 g/L, and 0.5 g/L: 0.1 g/L. The mass of the kaolin was systematically measured at three time points: 0, 15, and 30 min after dispersion. This was achieved by pipetting 10 mL of the suspension from the surface, which was at a depth of 3.0 cm of test tube. The 10 mL pipette was evaporated by heating with a magnetic stirrer at 40−50 °C until obtaining the dried residue, which was determined using a balance with four decimal digit precision.[9]

2.6. Reflection Efficiency of Coating Materials. The measurement of the intensity of light (photons) reaching the target per second is known as reflection efficiency in PPFD (μmol/m^2/s). Each 2 mL of the suspension sample was sprayed onto a microscope glass slide (2.5 cm in width and 7.5 cm in length) immediately (0 min) after the preparation and 30 min after the preparation without shaking. Subsequently, the slide was subjected to a light source with adjustable light intensity, which was achieved by altering the distance between the slide and the light source, and this process was continued after the suspension had fully dried. The light that passed through the slide was quantified as PPFD; a light sensor was placed underneath the glass slide to perform this measurement. The approximate distance between light source and sensor for 2000, 1800, 1600, 1400, 1200, 1000, and 800 μmol/s/m^2 were 47, 53, 58, 63, 70, 78, and 83 cm, respectively.

2.7. The Measurement of pH and Surface Charge. Kaolin was combined with different adjuvants as in the weight content experiment, and pH value was measured by pH meter with 2 decimal places. The kaolin clays were dispersed at 30 g/L in deionized water to measure the zeta potential using a Zetasizer Nano ZS (Malvern Instruments, UK) as well as the samples, including adjuvants such as PEG−PPG-PEG, PAA, and PSAMA.

3. RESULTS AND DISCUSSION

Minerals commonly utilized in agricultural applications, particularly in spray-on applications for coating plant leaves, serve a diverse range of functions. Therefore, the ideal clay for minimizing heat and drought stress should exhibit low thermal conductivity and high reflectivity. Another essential aspect is its particle size and water dispersibility as larger particles tend to settle rapidly, presenting challenges in spray applications.

3.1. Phase Identification and Particle Size. The X-ray diffraction analysis revealed that clays sourced from MaeThan (MT), Ranong (RN), Lampang (LP), Ceramic-Lampang (C-LP), Narathiwat (NRTW), Imerys, and SCG contained diverse minerals, which notably included kaolinite, quartz, zeolite, Illite, muscovite, and the annite phase. A detailed breakdown of these minerals can be found in Figure 2 as qualitative profiles and is summarized in Table 1 as quantitative values.

Moreover, the examination of particle images revealed that clays originating from SCG, RN, LP, and NRTW had larger particle dimensions in contrast to those originating from C-LP, Imerys, and MT. C-LP, Imerys, and MT clay powders displayed an average particle size ranging from 2.7 to 4.8 μm, clays from SCG, RN, LP, and NRTW possessed an average particle size exceeding 6 μm by SEM (Figure SI1), which may result in heightened sedimentation and difficulties in spray applications. Consequently, the study's focus narrowed down to clays from C-LP, Imerys, and MT.

Furthermore, a semiquantitative assessment of the mineral phases indicated that Imerys consisted of pure kaolin. With its pure kaolinite composition, characterized by nonconductivity and reasonably sufficient reflectivity, Imerys is therefore well-suited for spray-on applications on plant leaves, but it is commercially available. Regarding C-LP and MT, the presence of quartz, despite its higher thermal conductivity compared to the kaolinite phase, results in reduced insulating properties. However, the heat conductivity compensates for its relatively high reflectivity. This makes C-LP and MT viable options for mitigating heat and drought stress when applied to plants. As the composition of C-LP, it is worth considering that annite is an Fe-rich member of the mica group and has similar properties with muscovite (Al-rich).[35] While muscovite is noncoloring of the constituent elements and thin sheets. As the presence of quartz, the stability range of annite becomes more limited[36] (Table 1, Entry 1). On the other hand, it has been reported that the presence of the muscovite phase significantly influences the degree of dynamic recrystallization in quartz when the muscovite content falls below 25% of the quartz composition.[37] Consequently, the composition of the MT powder is hereby estimated to be approximately 16% (Table 1, Entry 3). Up to this point, C-LP and MT have been under consideration due to their absence of zeolite phases and their association with quartz phases, especially when compared with the pure kaolinite of Imerys.

Additionally, Brunauer−Emmett−Teller (BET) theory quantifies the surface area of solid porous materials, offering vital insights into their physical structure and interaction with the surrounding environment, particularly gases. This principle operates on the assumption that the particles within the material are spherical and monodisperse. (Table 1). Herein, considering the kaolinite composition, Imerys, composed entirely of kaolinite, displayed the highest BET value of 18.4 m^2/g, along with a particle size of 2.7 ± 0.5 μm. NRTW contained 85% kaolinite and exhibited a notable BET value of approximately 15.8 m^2/g with a particle size of 6.1 ± 1.5 μm. The trend can be attributed to the relatively smaller particle sizes, which contribute to the increased specific surface areas of these materials. It is notable that the particle sizes of C-LP, MT, and LP exhibited a tendency toward 4.8 ± 1.4 μm, 4.8 ± 1.0 μm, and 7.2 ± 1.9 μm, resulting in BET values of 12.6 11.4, and 9.9 m^2/g, respectively. In contrast, SCG and Ranong
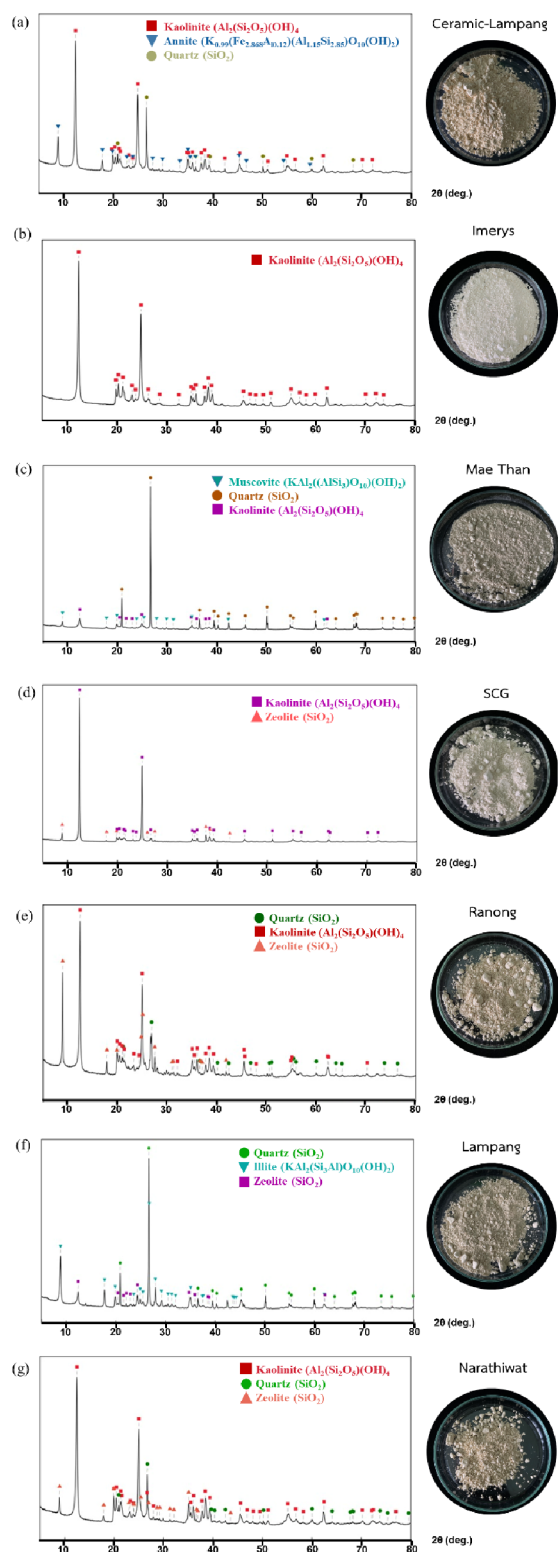
Figure 2. Determination of mineralogical composition of regional kaolin clay powder by XRD pattern and their average size of flake: (a) Ceramic-Lampang, (b) Imerys, (c) MaeThan, (d) SCG, (e) Ranong, (f) Lampang, and (g) Narathiwat.

displayed BET values of 7.9 and 13.2 m^2/g. As a result, the clays were analyzed without any treatment, which may potentially lead to the aggregation of clay particles, retention of mineral impurities, and dissolution of the external layers.[38] It is worth noting that except for LP, all natural clays were
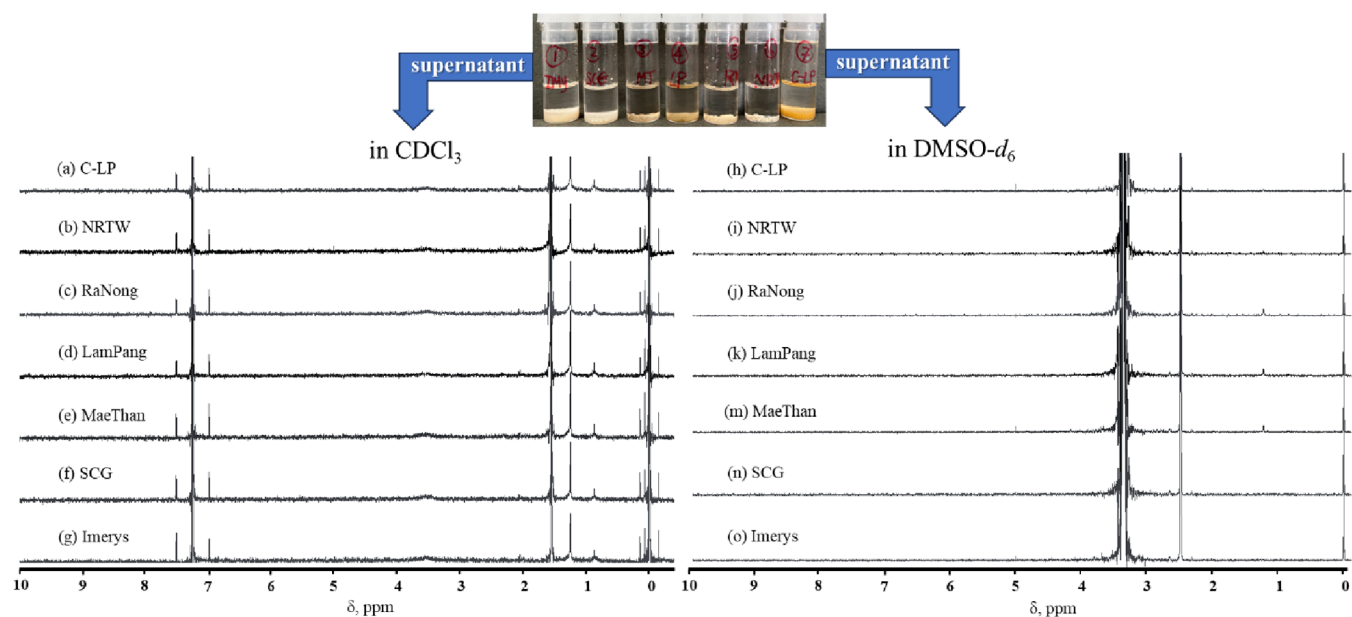
primarily composed of kaolinite as their major mineral component. However, these clays may indeed contain mineral impurities, such as quartz, illites, muscovite, and zeolite. These natural impurities can significantly affect the surface absorption value, and they are a key factor to consider in various applications, such as catalytic activity, moisture retention, and particularly dissolution rates.

As mentioned above, following the quantification of the inorganic content, the analysis expanded to include the determination of organic compound impurities. This comprehensive approach was ensured that all sedimentation behavior is attributed to the inorganic phase of the clays and their natural grain structures, and the supernatant of the clay solution was subjected to examination for organic compounds using ^{1}H NMR, as depicted in Figure 3. The supernatant (solution layer) was collected and subsequently evaporated, in both deuterium organic solvent such as chloroform (CDCl$_3$) and dimethyl sulfoxide (DMSO-d_6). Nonpolar solvent CDCl$_3$ and aprotic solvent DMSO-d_6 were employed for the analysis. As the ^{1}H NMR spectra, CDCl$_3$ exhibited peaks at 7.26 ppm, hexane peaks at 0.88 and 1.26 ppm, and water at 1.55 ppm. Similarly, in DMSO-d_6, the solvent peaks were observed at 2.50 ppm, hexane peaks at 0.85 and 1.25 ppm, and water at 3.33 ppm. From the result, no other organic compounds were detected in the analysis, indicating that all commercial and mined kaolinites, including C-LP (Figure 3a,h), NRTW (Figure 3b,i), RN (Figure 3c,j), LP (Figure 3d,k), MT (Figure 3e,m), SCG (Figure 3f,n), and Imerys (Figure 3g,o), were pure and noncontaminated with organic constituents. So far, the presence of hexane has been attributed to the dried clay's gas absorption as well as water moiety after the filter press process.

3.2. Sedimentation of the Clay Suspensions. According to spraying and coating applications, colloidal suspensions of mineral clays tend to precipitate easily when immersed in water, primarily attributed to the flocculation and gravity settling tendencies of kaolinite. Among the various sizes of the clay grains, our emphasis was on achieving homogeneous suspensions and ensuring the long-lasting diffusion of particles in the solution. Consequently, we paid our attention to the top three mineral phases with the smallest particle sizes (2−5 μm): Imerys, MT, and C-LP to emphasize the phenomena. Therefore, turbidity measurements of suspension could be utilized to evaluate the diffusion capability of colloidal particles in aqueous. We employed UV−vis spectroscopy to examine the variations in transmittance percentages (%T) at different clay suspension concentrations, specifically 10 g/L, 20 g/L, and 30 g/L within 40 min monitoring (Figure 4c−e). High transmittance intensity indicated rapid settling at the bottom (Figure 4a), whereas low transmittance intensity suggested increased stability of colloidal particles in the supernatant (Figure 4b). In this study, deionized water was marked as the reference with 100%T, and Imerys served as the pure-grade positive reference. The results revealed that C-LP at a concentration of 30 g/L exhibited a notably high transmittance value at 35%T (±3.8) within 40 min, indicating rapid precipitation of particles. Conversely, MT exhibited a transmittance pattern that closely resembled that of Imerys, which showed variations within 0.04%T. (Figure 4g,h). The concentration of the clay suspension appears to significantly influence settling behaviors, with particular attention given to the condition at 30 mg/L (Figure 4f−h). C-LP exhibited a strong inclination toward higher sedimentation in all conditions when compared to MT, specifically at 35%T

Table 1. Determination of Mineralogical Composition of Regional Kaolin Clay by X-Ray Diffraction Analysis and Average Size of Flake

		phases (wt %), quantitative analysis via XRD						SEM	BET
entry	sample	kaolitine $(Al_2(Si_2O_5)(OH)_4)$	quartz (SiO_2)	zeolite (SiO_2)	illite $(KAl_2(Si_3Al)O_{10}(OH)_2)$	muscovite $(KAl_2((AlSi_3)O_{10})(OH)_2)$	annite $(K_{0.99}(Fe_{2.868}A_{10.12})(Al_{1.15}Si_{2.85})O_{10}(OH)_2)$	average size (μm)	surface area (m^2/g)
1	Kaolin 1 (Ceramic-Lampang)	60	31	-	-	-	9	4.8 ± 1.4	12.6
2	Kaolin 2 (Imerys)	100	-	-	-	-	-	2.7 ± 0.7	18.4
3	Kaolin 3 (MaeThan)	45	48	-	-	8	-	4.8 ± 1.0	11.4
4	Kaolin 4 (SCG)	74	-	26		-	-	6.7 ± 3.0	7.9
5	Kaolin 5 (Ranong)	73	11	16	-	-	-	10.6 ± 5.3	13.2
6	Kaolin 6 (Lampang)	-	66	1	33	-	-	7.2 ± 1.9	9.9
7	Kaolin 7 (Narathiwat)	85	12	3	-	-	-	6.1 ± 1.5	15.8

Figure 3. ^1H NMR spectra of supernatant (upper layer solution) of Kaolin clay solution in each region of this case study in $CDCl_3$ (a-g) and DMSO-d_6 (h-o) at 400 MHz.

(±3.8) for concentrations of 30 g/L (Figure 4i), 19.5%T (±2.2) for 20 g/L (Figure 4j), and 6%T (±1.4) for 10 g/L (Figure 4k). It was assumed that flocculation is independent of kaolinite concentration and type within the range examined. Flocculation is faster at higher concentrations of kaolinite and the flocs are large and settle rapidly, especially C-LP. Imerys, which is commercially available, showed excellent disperse ability as well as MT. It was suggested that Imery and MT suspensions exhibited low transmittance due to their small particle size and high purity, in contrast to C-LP. Therefore, MT will be a potential candidate for the next quantitative study at 30 g/L of concentration.

As with the aforementioned results, it is evident that we have effectively optimized the sedimentation behavior in terms of precipitation rate for each clay solution. Nevertheless, our primary focus remains on quantifying the amount of dispersed particles in the supernatant, a critical consideration for assessing their potential in coating and spraying applications. To address this, we introduced a range of adjuvants, including

both monomers and polymers, with the aim of investigating their influence on enhancing the dispersion of the clay solution. Consequently, we systematically introduced various commercial types and quantities of these adjuvants to pinpoint the optimal polymer concentration. The chemical structures of these adjuvants are illustrated in Figure 1, categorized as follows: two monomers, taurine and zwitterion; four polymers, PEG−PPG-PEG, PDDA, PAA, and PSAMA.

3.3. Weight Content of the Clay Suspensions (Dispersity Improvement). In pursuit of practical kaolin solution spraying, the measurement of the weight content was essential for quantification. In a previous report, it was observed that kaolin-sprayed mangoes showed an increase of approximately 40% of their offsprings. To cover all leave of the entire canopy uniformly coated (without any adjuvant), 700 mL of a 60 g/L concentration of suspension was needed by power spray.[28] To the best of our knowledge, the practical requirement for spraying a solution from a 20L tank is estimated to take approximately 30 min. Herein, we examined
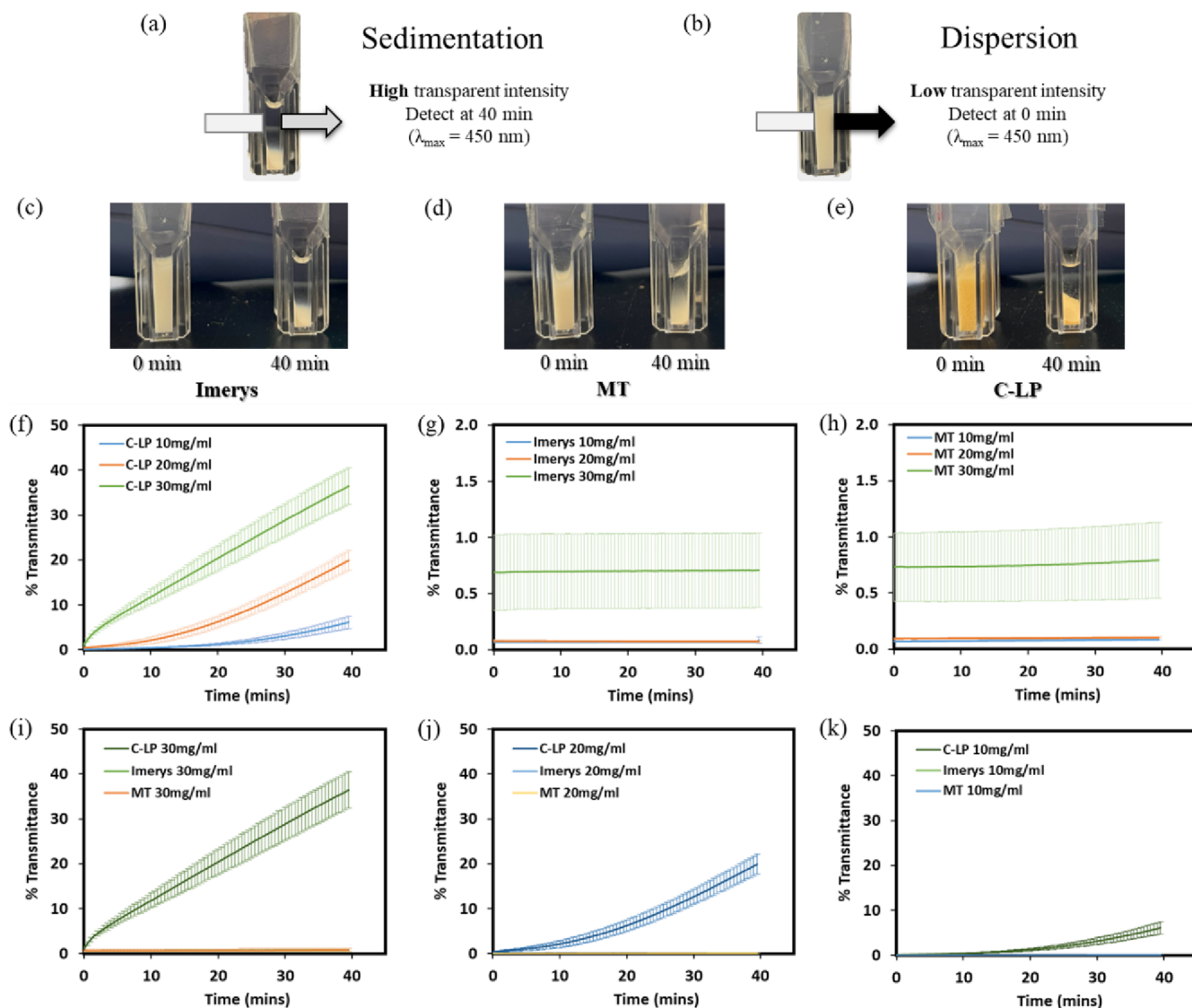
Figure 4. Sedimentation observation of kaolinite clays by transmittance percentage by UV−vis spectroscopy for 40 min (n = 3).

the impact of various polymer types and their optimal concentrations of MT, specifically at 30 g/L. The weight content was collected at a height of 3 cm from the suspension surface and subsequently dried to determine the precise amount of dispersed kaolinite pellets (Figure 5a) during 0, 15, and 30 min. In the absence of an adjuvant, the kaolin content in the solution part was observed to decrease to 40% weight, signifying that roughly 60% of kaolinite particles precipitated after 30 min (Figure 5b, i). Furthermore, it was noted that at higher concentrations, the flocculation of kaolinite occurs more rapidly, leading to the formation of larger. While, adding a small molecule such as taurine at a concentration of 0.5M, it was observed that 14% of dispered content (Figure 5bii), whereas zwitterion was 2% (Figure 5biii), indicating the lowest remaining content. Based on these findings, it became evident that the electrostatic charge of the amphiphilic molecule did not assist in the prevention of flocculation and precipitation; rather, it may influence the instability of colloidal particles. Ma grop reported that the clay particle orientation in pure water formed a dispersion structure with face-to-face repulsion, which induced the aggregation mode.[38] The surface of kaolinite platelets is negatively charged under ultrapure water

chemistry conditions. The ionic strength circumstance could improve the stability; however, it was reported that the kaolins in brine solution, especially NaCl, and concentration also acclerated the sedimentation related to the stability of the colloidal.[25]

Next, the PEG−PPG-PEG is a block copolymer and is known as an excellent surfactant composing terminal polar PEG fragments and a nonpolar PPG fragment in the center. In this study, the triblock PEG−PPG-PEG was used as a noncharge adjuvant and investigated at concentrations of 0.1 g/L, 1.0 g/L, and 3.0 g/L. From the result during 30 min, it was shown that the kaolin with 0.1 g/L PEG−PPG-PEG was massively precipitated (65%) and the remaining dispersed kaolin only 35% weight (Figure 5civ), which is more than nonadjuvant (Figure 5ciii). On the other hand, the mixture of adjuvant at 1.0 and 3.0 g/L improved kaolin content dispersion approximately 48% and 47%, respectively (Figure 5ci and ii). If cost consumption was considered, it seems that 1.0 g/L of PEG−PPG-PEG was the optimized condition. As the result, it is found that the triblock polymer of PEG−PPG-PEG is an interesting candidate, while another random polymer with disordered structure such as poly(ethylene glycol-*ran*-propy-
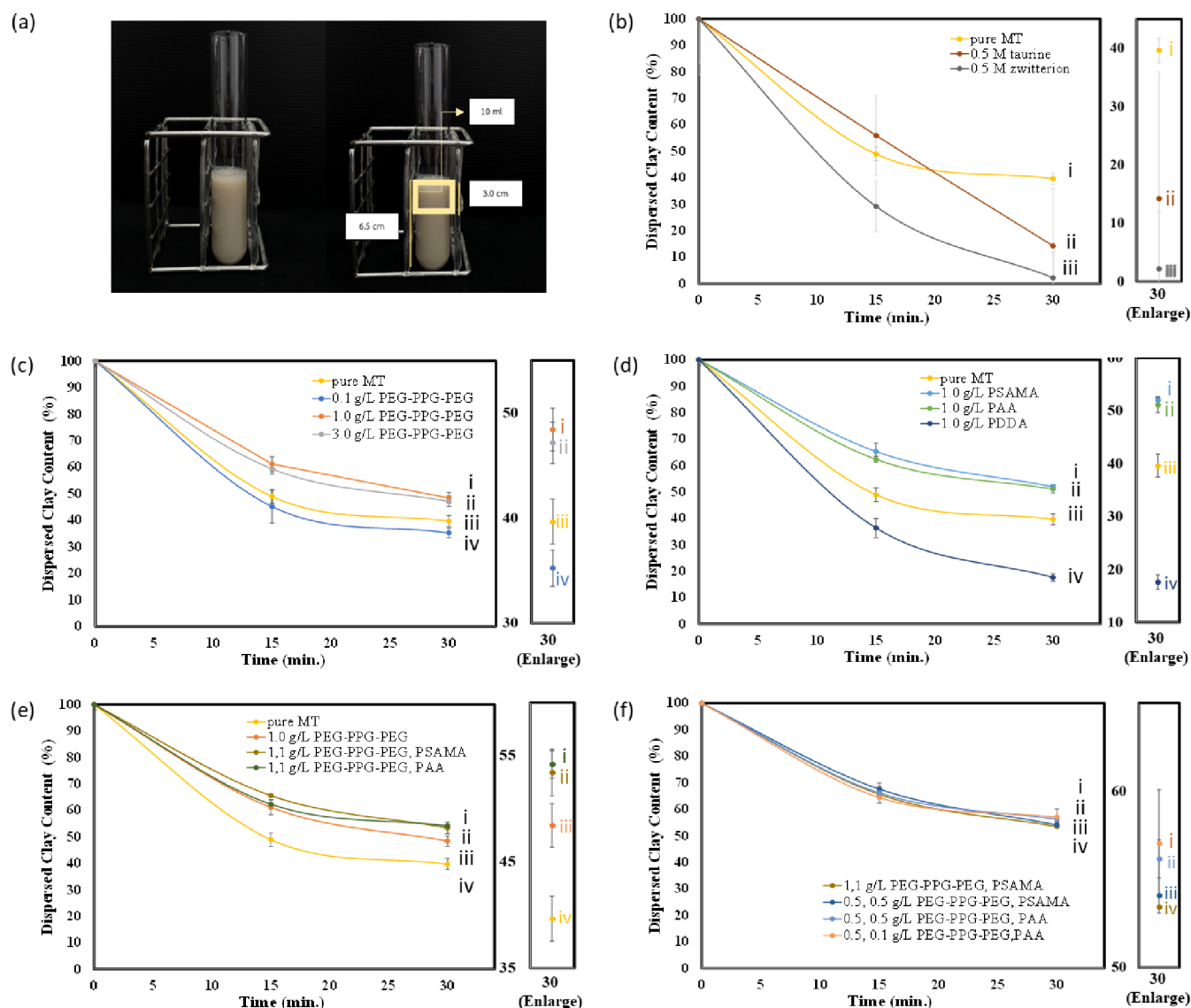
Figure 5. Clay weight in suspension layer with time dependence and a series of adjuvants. Each enlarged scale at 30 min is inserted.

lene glycol) is not proper for delaying the sedimentation. So the properties of such copolymer could be expressed as averaged properties of PEG and PPG polymers without any characteristic features of the structural fragments along the copolymer chain. Then, a couple of charged polymers such as positively charged PDDA and negatively charged PSAMA and PAA, were investigated. At 1.0 g/L adjuvant, the negatively charged polymers, both PSAMA and PAA, behaved to improve the dipersion of kaolin weight 52% and 51%, respectively (Figure 5di and ii). In contrast, a positive PDDA was the worst circumstance, resulting in 18% kaolin content (Figure 5div). Therefore, it may conclude that the negative charge of the polymer may contribute to prolonging the stability of the kaolin particles in suspension.

To better understand how the combination works, PEG−PPG-PEG and negatively charged PSAMA and PAA were blended in a rational 1:1 g/L ratio (Figure 5e). As the 1.0 g/L of PEG−PPG-PEG was the optimized condition, when combined with 1.0 g/L of PAA, it was observed to improve the dipersion of kaolin weight from 48% of single PEG−PPG-PEG adjuvant to 54% of double adjuvants (Figure 5ei).

Furthermore, the occurrence of combining 1.0 g/L PSAMA and 1.0 g/L PEG−PPG-PEG resulted in 53% kaolin weight, as observed (Figure 5eii). Subsequently, the ratios of two combination adjuvants as 0.5/0.1 g/L, 0.5/0.5 g/L, and 1/1 g/L were evaluated. PEG−PPG-PEG/PSAMA 1/1 g/L provided 53% of dispersed kaolin (Figure 5fiv) while at 0.5/0.5 g/L was shown 54% (Figure 5fiii). Additionally, when comparing PEG−PPG-PEG/PAA ratios of 0.5/0.5 and 0.5/0.1 g/L, the depicted dispersion weights were 56% (Figure 5fii) and 57% (Figure 5fi), respectively. Based on the result, a series of the adjuvant ratios did not exhibit significant differences, implying that the ratio did not directly influence dispersion stability in this study. The combination of the two adjuvants did not lead to a 2-fold increase in the dispersion of kaolin weight, and the adjuvant ratio also did not impact such an effect. However, there was a notable ideation of using polymeric adjuvants presenting an improvement from 40% (no adjuvant) to a maximum of 57% (two adjuvants). This study suggests that polymeric adjuvants, including PEG−PPG-PEG, PSAMA, and PAA, positively influenced kaolinite

suspension, particularly the combination of PEG−PPG-PEG/PAA.

Our finding convinced the environmental benefits of utilizing local mining kaolin and sustainable adjuvants comparable with control (without polymer adjuvants). The combination of two adjuvants at a concentration of 30 g/L resulted in a significant enhancement in the dispersed kaolin weight, with an increase of up to 17%, highlighting the remarkable benefits of this approach.

For further emphasis on suspension behavior, visualization was proposed based on the results of dispersed clay weight, as shown in Figure 6. A novel finding was that negatively charged
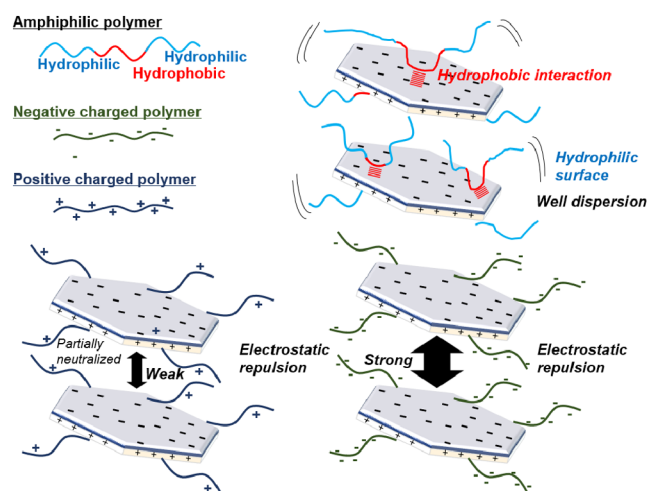

Figure 6. Proposed role of adjuvants in kaolin suspension includes enhancing the dispersion and stability of the kaolin particles.

adjuvants contributed to the exfoliation of kaolin particles in water, regardless of the specific chemical structures, density, or molecular weight. Conversely, positively charged adjuvants tended to promote particle packing and precipitation. Furthermore, the role of neutral amphiphilic adjuvants in kaolin suspension was significant in enhancing the dispersion and stability of the kaolin particles. This suggests that the impact was enhanced by the hydrophobicity of the amphiphilic polymer.

In light of this study, addressing the limitations associated with using locally sourced mining clays and sustainable adjuvants for coating applications remains a significant challenge. However, the pressing concern lies in achieving facile and large-scale production. Further modification of mining kaolin appears to be challenging, as well as the usage of adjuvants due to their impact on production costs. Therefore, the study will be suggested on determining the optimal amount of adjuvant with satisfied dispersion and ensuring an approached market. Additionally, we would challenge the synthesis of alternative adjuvants based on poly(butylene succinate) derivatives for mass production. Furthermore, we plan to further investigate the practical challenges of citrus cultivation, building upon the remarkable results obtained in collaboration with specialized partners in the agriculture field.

3.4. Reflection Efficiency of Coating Materials. The developed coating materials play a crucial role in exploring the significance of postharvest technology and sustainable agriculture aspects. However, the actual cultivation of fruits, including yield and quality, requires extensive time and space in the field, which exceeds the scope of polymer science.

Therefore, the evaluation of the photosynthesis system (PPFD) is employed to validate the potential of coating materials in terms of light reflection efficiency. As our knowledge, the practical demand for spraying a mining clay solution of 20L tank is estimated to take 30 min. Herein, we investigated the response of light reflection after spraying the kaolin suspensions on the glass substrate for 30 min according to the practical state. The experimental demonstration of the light reflection with side and top views is shown in Figure 7a. The source light intensity ($PPFD_o$) was varied across different feeding units as the following set was set at 800, 1000, 1200, 1400, 1600, 1800, and 2000 $PPFD_o$. Subsequently, the light intensity passing through the glass was determined in terms of PPFD. A screening of the suspension without additives were conducted at initial 0 min and at 30 min (Figure 7b) in order to observe the difference clay content of suspension. The obtained intensity was higher after 30 min, which indicated that the content of kaolin was less than at initial assuming the high aggregation of kaolin during time passed. Targeting citrus tree leaves and fruit desired PPFD region between 650 and 1000 $\mu mol/s/m^2$,[29,30] the result indicated that the desired PPFD region within 30 min were achieved with specific $PPFD_O$ at 1200 and 1400. Therefore, the various conditions of suspension with adjuvants were investigated and optimized at source light intensities of 1200 and 1400 $PPFD_o$ (Figure 7c). It was found that suspension conditions presented the acceptable reflection efficiency wihtin the desired PPFD region (650−1000 $\mu mol/s/m^2$). However, the stable tendency was found in one adjuvant system of PEG−PPG-PEG better than PAA and PSAMA considering the deviation. Regarding two adjuvant system, four conditions showed excellence acceptable region without significance: 1/1 g/L PEG−PPG-PEG/PAA, 0.5/0.5 g/L PEG−PPG-PEG/PSAMA, 0.5/0.5 g/L PEG−PPG-PEG/PAA, and 0.5/0.1 g/L PEG−PPG-PEG/PAA.

Considering that the light intensity increased after 30 min, it is possibly related to the light penetration. Assuming low light detection, a high content of kaolin might be spread on the substrate. Therefore, the images of coated glass substrates are presented in Figure 8, illustrating three conditions: spraying with only adjuvants (Figure 8a), kaolin suspension without adjuvant (Figure SI2), kaolin suspension with one adjuvant (Figure 8b), and double adjuvant system (Figure 8c). Based on the results, it was observed that only the adjuvant did not contribute to light reflection due to its complete transparency. Additionally, the kaolin suspension with 1 g/L PSAMA showed a high void surface, indicating a lack of smoothness and flexibility during the coating. This observation was similar to the findings with 1 g/L PAA and no adjuvant. On the contrary, under other conditions, nearly full coverage was observed, presenting an opportunity to improve the reflection efficiency of coating materials. These conditions include 1 g/L PEG−PPG-PEG, 0.5/0.5 g/L PEG−PPG-PEG/PSAMA, 1/1 g/L PEG−PPG-PEG/PAA, 0.5/0.5 g/L PEG−PPG-PEG/PAA, and 0.5/0.1 g/L PEG−PPG-PEG/PAA.

3.5. The Measurement of pH and Surface Charge. Kaolinite mineral is composed of layered silicates with a hexagonal structure, and its main chemical component is $Al_2Si_2O_5(OH)_4$. Kaolinite predominantly featured negatively charged faces (SiO_2) and positively charged edges (Al_2O_3). The nonuniform charge distribution typically promotes particle aggregation, which is the limitation of utility. Surface force measurements revealed that the silica tetrahedral face of kaolinite is negatively charged at pH > 4, whereas the alumina
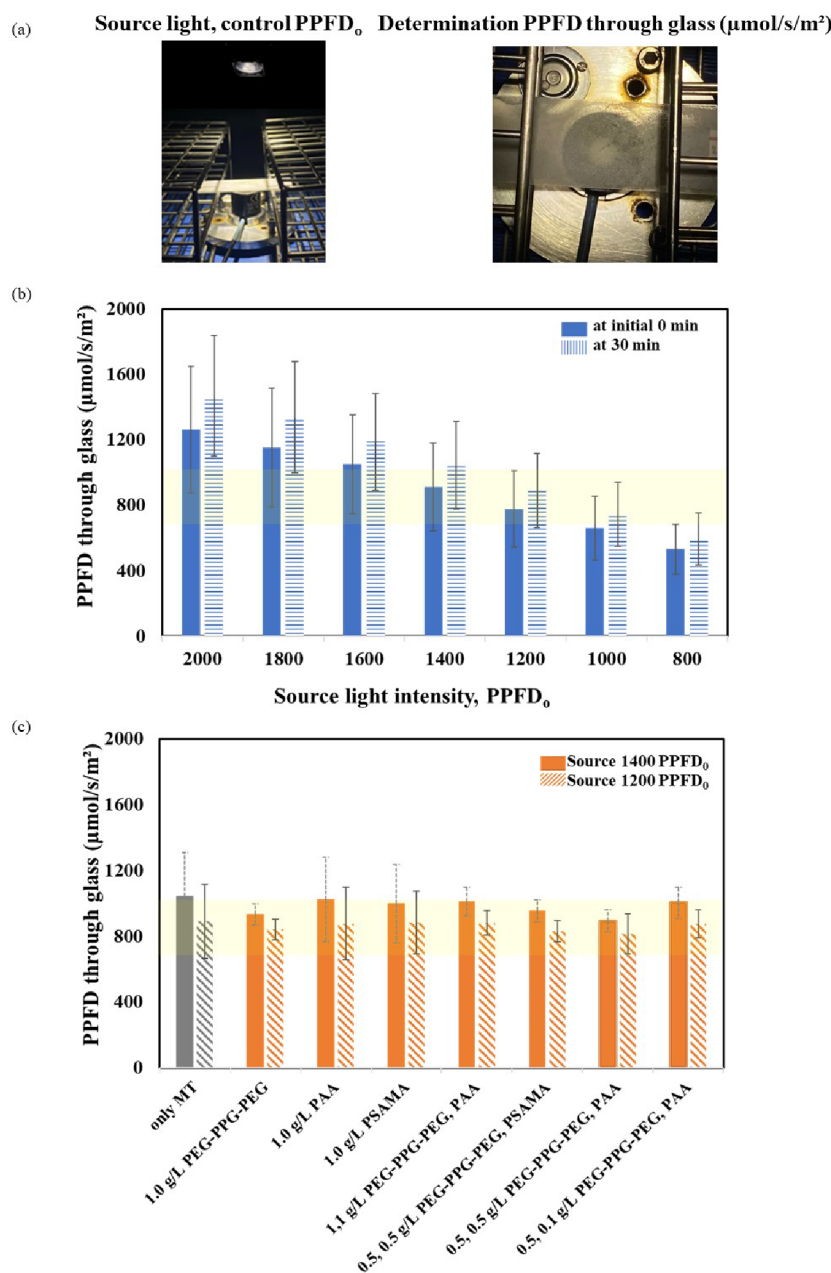
Figure 7. Measurement of total number of photons on glass substate by photosynthetic photon flux density (PPFD) with various light source intensity (a) and series of clay coating on substrate at initial 0 min and after 30 min dispersion (b), with diverse adjuvants after 30 min dispersion by 1200PPFD$_0$ and 1400PPFD$_0$ (c).

octahedral face of kaolinite is positively charged at pH < 6 and negatively charged at pH > 8.[36] In this report, we also analyzed the zeta potential as an indicator for a potential adjuvant material as well as the pH level. The zeta potential was investigated, as illustrated in Figure 9a. The zeta potential (ZP) measurements for commercial and pure grades of kaolin were as follows (SD): Imerys −36 mV (±4.7), C-LP −29 mV (±4.7), and MT −28 mV (±1.0) (Figure 9aI−III). While adding an adjuvant, the ZP value of 1 g/L PEG−PPG-PEG was −23 mV (±1.8) (Figure 9aIV), which tends to be decreased. With double adjuvants, they were slightly increased, comparing MT without adjuvant as follows: 0.5/0.5 g/L PEG−PPG-PEG/PAA was −30 mV (±1.2) (Figure 9aV), 0.5/0.5 g/L PEG−PPG-PEG/PSAMA was −27 mV (±2.1) (Figure 9aVI), 0.5/0.1 g/L of PEG−PPG-PEG/PAA was

−31 mV (±2.9) (Figure 9aVII), and 0.5/0.1 g/L of PEG−PPG-PEG/PSAMA was −31 mV (±1.0) (Figure 9aVIII). The results indicated that the zeta potential slightly increased upon the addition of negatively charged components but decreased upon the incorporation of amphiphilic PEG−PPG-PEG. This suggests that the effect of the adjuvant did not dramatically alter the surface charge of the kaolin particles. The range of zeta potential (−23 mV to −31 mV) may not represent a significant change, but the overall stability remained negative. Subsequently, the pH levels were examined to explore any potential correlation. It is advisable to use a coating suspension with a pH that does not induce acidity. According to literature, citrus plant is well grown in soil with a neutral pH between 6 (lightly acid) and 7. High alkaline soil hinders the absorption of iron, magnesium, and zinc, which are crucial for chlorophyll
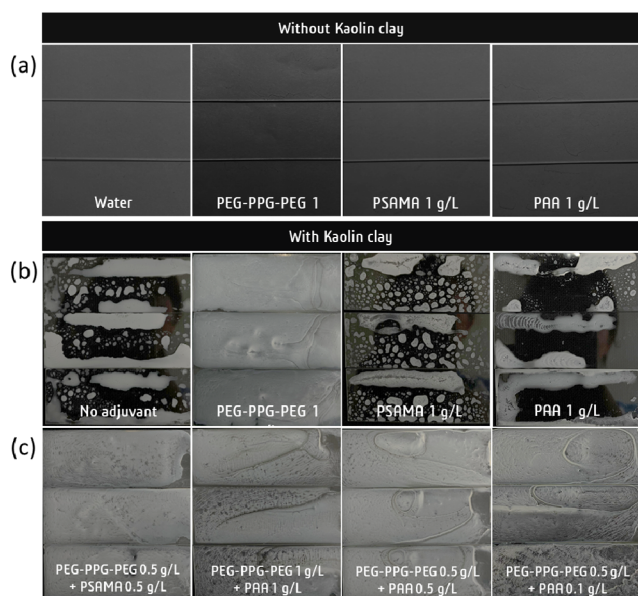
Figure 8. Observation of coated substrate by only adjuvants (a), kaolin suspension with one adjuvant system (b), and with two adjuvant system (c).

production.[39] In these experiments, MT without adjuvant and with the noncharge PEG−PPG-PEG were presented at pH 6.7 (Figure 9b1,3), while the addition of the small molecule taurine resulted in a pH of 5.4 (Figure 9b2). In the case of the double adjuvant system, the pH slightly increased according to the amount of PAA or PSAMA. Specifically, 0.5/0.1 g/L PEG−PPG-PEG/PAA was shown at pH 7.4, which was almost neutral condition (Figure 9b4). There was pH 7.9 for 0.5/0.5 g/L PEG−PPG-PEG/PSAMA (Figure 9b7), pH 8.3 for 0.5/0.5 g/L PEG−PPG-PEG/PAA (Figure 9b5), pH 8.3 for 1/1 g/L PEG−PPG-PEG/PSAMA (Figure 9b8), and pH 8.3 for 1/1 g/L PEG−PPG-PEG/PAA (Figure 9b6). All standard

deviations were approximately in the range of ±0.03 to ±0.1, indicating a high level of accuracy. In the current observation, it was noted that a lower amount of negatively charged components in the double adjuvant system provided neutral pH and surface charge, particularly 0.5/0.1 g/L rationing one. Although the contribution of the adjuvant system in dispersed kaolin weight and effective light reflection were the primary considerations for candidates, the application utility also demonstrated promise. Maintaining a proper pH is incredibly important as soil nutrients play a vital role in every aspect of the tree's functions, including growth, flowering, fruiting, immune system, and water retention.[26]

4. CONCLUSION

The systematic investigation into the impact of adjuvants, encompassing both organic molecules, a polymeric adjuvant, and double polymeric adjuvants, on the sedimentation behavior of clay suspensions has provided valuable insights. The incorporation of dual adjuvants, comprising both neutral and amphiphilic polymers such as PEG−PPG-PEG and negatively charged polymers such as PAA and PSAMA, demonstrated a noteworthy ability to effectively retard sedimentation. This resulted in an approximately 17% increase of kaolin weight after 30 min. The ratio of 0.5 g/L of neutral to 0.1 g/L of negatively charged adjuvants reached the optimized condition, highlighting not only enhanced uniformity of the coated surface but also reduced cost consumption. This finding demonstrates the potential for enhancing coating materials' reflective efficiency by incorporating polymer adjuvants in the 650−1000 μmol/s/m^2 PPFD range while maintaining a neutral pH level. As we project into the future, this insight holds promise for guiding the design of synthetic polymers, offering cost-effective and efficient solutions for various applications.
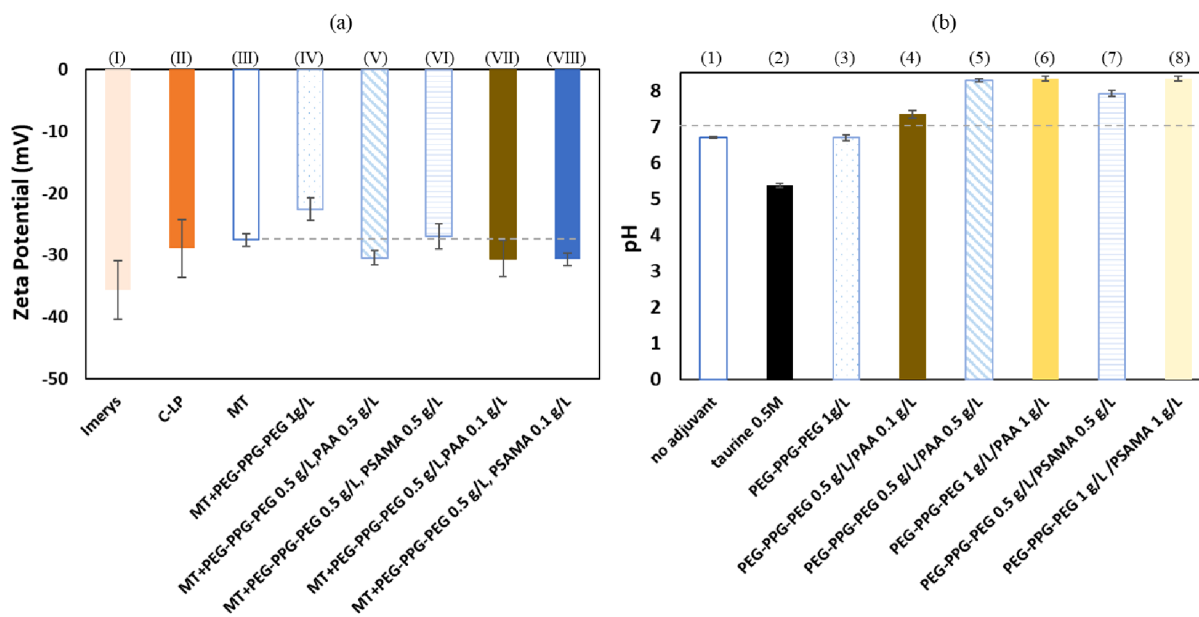

Figure 9. Zeta potential of kaolinite clays 30 g/L (a), Imerys (I), C-LP (II), MT (III,(1)) and MT in the presence of PEG−PPG-PEG (IV, (3)), PEG−PPG-PEG/PAA (V,VII,(4),(5),(6)), and PEG−PPG-PEG/PSAMA (VI,VIII,(7),(8)) and pH of MT 30 g/L suspension with adjuvants (b) during 0−30 min.

ASSOCIATED CONTENT

Supporting Information

The Supporting Information is available free of charge at https://pubs.acs.org/doi/10.1021/acsomega.4c00539.

SEM images of Kaolin grains. Photos of coated substrate by spraying of Kaolin solution without adjuvant (PDF)

AUTHOR INFORMATION

Corresponding Authors

Nalinthip Chanthaset − *Materials Science Division, Nara Institute of Science and Technology, Nara 630-0192, Japan;* Email: nalin@ms.naist.jp

Hiroharu Ajiro − *Materials Science Division, Nara Institute of Science and Technology, Nara 630-0192, Japan; Data Science Center, Nara Institute of Science and Technology, Nara 630-0192, Japan;* orcid.org/0000-0003-4091-6956; Email: ajiro@ms.naist.jp

Kanapol Jutamanee − *Department of Botany, Faculty of Science, Kasetsart University, Bangkok 10900, Thailand;* Email: faaskpj@ku.ac.th

Authors

Nichagarn Greetatorn − *Department of Botany, Faculty of Science, Kasetsart University, Bangkok 10900, Thailand*

Oratai Jongprateep − *Department of Materials Engineering, Faculty of Engineering, Kasetsart University, Bangkok 10900, Thailand*

Complete contact information is available at:
https://pubs.acs.org/10.1021/acsomega.4c00539

Notes

The authors declare no competing financial interest.

ACKNOWLEDGMENTS

REFERENCES

(1) Christopoulos, M.; Ouzounidou, G. Climate Change Effects on the Perceived and Nutritional Quality of Fruit and Vegetables. *J. Innovation Econ. Manage.* 2021, 34, 79−99.

(2) Sugiura, T.; Sakamoto, D.; Koshita, Y.; Sugiura, H.; Asakura, T. Changes in locations suitable for satsuma mandarin and tankan cultivation due to global warming in Japan. *Acta Hortic.* 2016, 1130, 91−94.

(3) Sugiura, T.; Yokozawa, M. Impact of global warming on environments for apple and satsuma mandarin production estimated from changes of the annual mean temperature. *J. Jpn. Soc. Hortic. Sci.* 2004, 73, 72−78.

(4) Sugiura, T.; Kuroda, H.; Sugiura, H. Influence of the current state of global warming on fruit tree growth in Japan. *J. Jpn. Soc. Hortic. Sci.* 2007, 6, 257−263.

(5) Thomas, A. L.; Muller, M. E.; Dodson, B. R.; Ellersieck, M. R.; Kaps, M. A kaolin-based particle film suppresses certain insect and fungal pests while reducing heat stress in apples. *J. Am. Pomol. Soc.* 2004, 58, 42−51.

(6) Glenn, D. M. The mechanisms of plant stress mitigation by kaolin-based particle films and applications in horticultural and agricultural crops. *HortScience* 2012, 47, 710−711.

(7) Gualtieri, M. L.; Gualtieri, A. F.; Gagliardi, S.; Ruffini, P.; Ferrari, R.; Hanuskova, M. Thermal conductivity of fired clays: Effects of mineralogical and physical properties of the raw materials. *Appl. Clay Sci.* 2010, 49 (3), 269−275.

(8) AbdAllah, A. Impacts of kaolin and pinoline foliar application on growth, yield and water use efficiency of tomato (Solanum lycopersicum L.) grown under water deficit: A comparative study. *J. Saudi Soc. Agric. Sci.* 2019, 18, 256−268.

(9) Cantore, V.; Pace, B.; Albrizio, R. Kaolin-based particle film technology affects tomato physiology, yield, and quality. *Environ. Exp. Bot.* 2009, 66 (2), 279−288.

(10) Obaje, S. O.; Omada, J. I.; Dambatta, U. A. Clays and their industrial applications: Synoptic Review. *Int. J. Sci.Technol.* 2013, 3, 264−270.

(11) Lima, S. A.; Murad, M. A.; Moyne, C.; Stemmelen, D. Electro-osmosis in kaolinite with pH-dependent surface charge modelling by homogenization. *An. Acad. Bras. Cienc.* 2010, 82 (1), 223−242.

(12) Tosca, N. J.; Masterson, A. L. Chemical controls on incipient Mg-silicate crystallization at 25 C: Implications for early and late diagenesis. *Clay Miner.* 2014, 49, 165−194.

(13) Palomino, A. M.; Santamarina, J. C. Fabric map for kaolinite: effects of pH and ionic concentration on behavior. *Clay Miner.* 2005, 53, 211−223.

(14) Letaief, S.; Detellier, C. Functionalization of the interlayer surfaces of kaolinite by alkylammonium groups from ionic liquids. *Clays Clay Miner.* 2009, 57, 638−648.

(15) Ta, E.; Detellier, C. Interlamellar grafting of polyols in kaolinite. *Clay Sci.* 2005, 12, 38−46.

(16) Tanaka, Y.; Okada, T.; Ogawa, M. Adsorption of tetrakis(p-sulfonatophenyl)porphyrin on kaolinite. *J. Porous Mater.* 2009, 16, 623−629.

(17) Ferreira, B. F.; Ciuffi, K. J.; Nassar, E. J.; Vincente, M. A.; Trujillano, R.; Rives, V.; de Faria, E. H. Kaolinite-polymer compounds by grafting of 2-hydroxyethyl methacrylate and 3-(trimethoxysilyl) propyl methacrylate. *Appl. Clay Sci.* 2017, 146, 526−534.

(18) Zhao, P.; Zhou, Q.; Yan, C.; Luo, W. Polyacrylic acid grafted kaolinite via a facile'grafting to' approach based on heterogeneous esterification and its adsorption for Cu2+. *Mater. Res. Express* 2017, 4, 035502.

(19) Kang, X.; Bate, B.; Chen, R.-P.; Yang, W.; Wang, F. Physicochemical and Mechanical Properties of Polymer-Amended Kaolinite and Fly Ash−Kaolinite Mixtures. *J. Mater. Civ. Eng.* 2019, 31 (6), 04019064.

(20) Kim, S.; Palomino, A. M. Polyacrylamide-treated kaolin: A fabric study. *Appl. Clay Sci.* 2009, 45, 270−279.

(21) Kang, X.; Xia, Z.; Chen, R.; Sun, H.; Yan, W. Effects of inorganic ions, organic polymers, and fly ashes on the sedimentation characteristics of kaolinite suspensions. *Appl. Clay Sci.* 2019, 181, 105220.

(22) Zhang, Y.; Long, M.; Huang, P.; Yang, H.; Chang, S.; Hu, Y.; Tang, A.; Mao, L. Intercalated 2D nanoclay for emerging drug delivery in cancer therapy. *Nano Res.* 2017, 10, 2633−2643.

(23) Mgbemene, C. A.; Akinlabi, E. T.; Ikumapayi, O. M. Influence of additives on kaolinite clay properties-applications, trends, and a case study. *Proc. Manuf.* 2019, 35, 1395−1399.

(24) García, K. I.; Quezada, G. R.; Arumiet, J. L.; Urrutia, R.; Toledo, P. G. Adsorption of Phosphate Ions on the Basal and Edge Surfaces of Kaolinite in Low Salt Aqueous Solutions Using Molecular Dynamics Simulations. *J. Phys. Chem. C* 2021, 125, 21179−21190.

(25) Yukselen, Y.; Kaya, A. Zeta potential of kaolinite in the presence of alkali, alkaline earth and hydrolyzable metal ions. *Water, Air, Soil Pollut.* 2003, 145, 155−168.

(26) Ma, X.-Y.; Kang, X.; Su, C.-X.; Chen, Y.-Q.; Sun, H.-M. Effects of water chemistry on microfabric and micromechanical properties evolution of coastal sediment: A centrifugal model study. *Sci. Total Environ.* 2023, 866, 161343.

(27) Ma, X.; Xia, Z.; Su, C. X.; Cheng, Y.; Yu, H.; Kang, X. Quantitative Evaluation of the Effects of Salt Concentration and pH

on the Self-Assembly of Kaolin Nanoplatelets. *Langmuir* **2023**, *39* (41), 14500−14510.

(28) Chamchaiyaporn, T.; Jutamanee, K.; Kasemsap, P.; Vaithanomsat, P.; Henpitak, C. Effects of Kaolin Clay Coating on Mango Leaf Gas Exchange, Fruit Yield and Quality. *Kasetsart J. Nat. Sci.* **2013**, *47*, 479−491.

(29) Zhang, J.; Li, Q.; Qi, Y.-P.; Huang, W. L.; Yang, L.-T.; Lai, N.-W.; Ye, X.; Chen, L.-S. Low pH-responsive proteins revealed by a 2-DE based MS approach and related physiological responses in Citrus leaves. *BMC Plant Biol.* **2018**, *18* (188), 188.

(30) Pallozzi, E.; Tsonev, T.; Marino, G.; Copolovici, L.; Niinemets, U.; Loreto, F.; Centritto, M. Isoprenoid emissions, photosynthesis and mesophyll diffusion conductance in response to blue light. *Environ. Exp. Bot.* **2013**, *95*, 50−58.

(31) Chen, C. I.; Lin, K. H.; Huang, M. Y.; Yang, C. K.; Lin, Y. H.; Hsueh, M. L.; Lee, L. H.; Wang, C. W. Photosynthetic Physiology Comparisons between No Tillage and Sod Culture of Citrus Farming in Different Seasons under Various Light Intensities. *Agron* **2021**, *11* (9), 1805.

(32) Habermann, G.; Machado, E. C.; Rodrigues, J. D.; Medina, C. L. CO_2 assimilation, photosynthetic light response curves, and water relations of 'Pêra' sweet orange plants infected with Xylella fastidiosa. *Braz. J. Plant Physiol.* **2003**, *15* (2), 79−87.

(33) Ribeiro, R. V.; Machado, E. C.; Oliveira, R. F.; Pimentel, C. High temperature effects on the response of photosynthesis to light in sweet orange plants infected with Xylella fastidiosa. *Braz. J. Plant Physiol.* **2003**, *15* (2), 89−97.

(34) Ribeiro, R. V.; Machado, E. C.; Oliveira, R. F. Temperature response of photosynthesis and its interaction with light intensity in sweet orange leaf discs under non-photorespiratory condition. *Cienc. Agrotecnol.* **2006**, *30* (4), 670−678.

(35) Breiter, K.; Müller, A.; Leichmann, J.; Gabašová, A. Textural and chemical evolution of a fractionated granitic system: The Podlesí stock, Czech Republic. *Lithos* **2005**, *80*, 323−345.

(36) Eugster, H. P.; Wones, D. R. Stability relations of the ferruginous biotite, annite. *J. Petrol* **1962**, *3*, 82−125.

(37) Tokle, L.; Hirth, G.; Stünitz, H. The effect of muscovite on the microstructural evolution and rheology of quartzite in general shear. *J. Struct. Geol.* **2023**, *169*, 104835.

(38) Panda, K.; et al.et al. Colloids and Surfaces A. *Physicochem. Eng. Aspects* **2010**, *363*, 98−104.

(39) Inoue, H.; Okada, A.; Uenosono, S.; Suzuki, M.; Matsuyama, T.; Masaoka, Y. Does HLB Disease Prefer Citrus Growing in Alkaline Soil? *Jpn. Agric. Res. Q.* **2020**, *54* (1), 21−29.